RSC Advances

ROYAL SOCIETY OF CHEMISTRY

www.rsc.org/advances

Structure, stability, mechanical and electronic properties of Fe-P binary compounds by first-principles calculations

Jing Wu[a], XiaoYu Chong[a], Rong Zhou[a], YeHua Jiang[a], Jing Feng[b,*]

[a] *Faculty of Material Science and Engineering, Kunming University of Science and Technology, Kunming 650093, People's Republic of China*

[b] *School of Engineering and Applied Sciences, Harvard University, Cambridge, MA 02138, USA*

Abstract

The equilibrium crystal structure, stability, elastic properties, hardness and electronic structures of Fe-P binary compounds (Fe_3P, Fe_2P, o-FeP_1, o-FeP_2, FeP_2, m-FeP_4_1, o-FeP_4, m-FeP_4_2) are investigated systematically by the first principles calculations. The calculated Formation enthalpy is used to estimate the stability of the Fe-P binary compounds. The Fe_3P has the largest formation enthalpy as -44.950 kJ/mol and o-FeP_2 has the smallest as -78.590 kJ/mol. The elastic constants are calculated by the stress-strain method and the Voigt-Reuss-Hill approximation is used to estimate the elastic moduli. The mechanical anisotropy of Fe_xP_y compounds are studied by the anisotropic indexes and plotting 3D surface contour of Young's modulus. The electronic structures and chemical bonding characteristics of Fe-P binary compounds are interpreted by the band structures and density of states. Finally, the sound velocity and Debye temperatures of Fe-P binary compounds are discussed.

Keywords: Intermetallics; Phosphide; First principles calculations; Elastic properties; Electronic properties

1. Introduction

* Corresponding authors. Tel.: +1 6174964295; fax: +1 857 259 2445. E-mail addresses: jfeng@seas.harvard.edu

Iron - steel industry has been developing fast since the last century, which is a symbol for the modern industry. A common non-metal element such as phosphorus would form the enrichment region in casting process or some heat treatment condition, (For example, grain-boundary segregation). Phosphorus would combine with iron to form the Fe-P binary compounds including Fe_3P, Fe_2P, FeP, FeP_2, and FeP_4 according to Fe-P equilibrium phase diagram.[1] Moreover, phosphorus is usually considered hazardous to the properties of the steel. But the phosphorus existing in the steel is inevitable. In order to control the effect of phosphorus in the iron and steels, first of all, we should know the structure, stability and properties of the iron phosphides.

As a traditional industry, most researches about the properties of steels depended on the experimental discovery. Therefore, it is difficult to explore the performance of these compounds at electron-atomic level. The development of first-principle calculations based on density functional theory [2,3] has made it possible to get the fundamental properties with electron-atomic level or materials under the difficult experimental conditions. Nevertheless, only few reports on iron phosphides. Li et al. [4] calculated the elastic constants and formation enthalpy of Fe_2P by first principle pseudo-potential plane wave method. They have found that both of hexagonal and orthorhombic Fe_2P intermetallic compounds were ductile. The hexagonal structure was more stable than orthorhombic structure for Fe_2P. Chen et al. [5] investigated the magnetic property of Fe_2P. They understood the magnetic properties of the compound even under considerable high pressures above 5.0 GPa. Tobola et al. [6] investigated the magnetism and band structure of Fe_2P by neutron diffraction experiment and KKR-CPA calculation method. However, most physical and chemical properties of Fe-P binary compounds are rarely reported systematically as so far. In this paper, the stability, mechanical properties and electronic structures of all Fe-P binary compounds are

investigated and discussed for the first time with first-principle calculation method.

2. Calculation methods and models

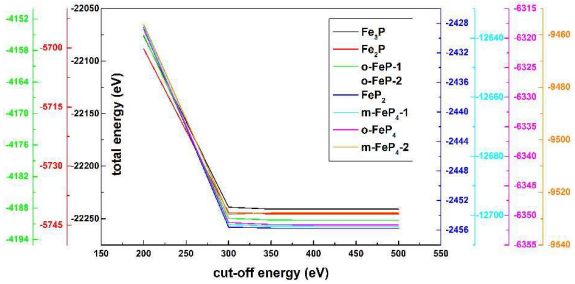

Fig. 1. Cut-off energy testing

The first-principle calculations of Fe-P compounds have been performed by density functioned theory (DFT) which is implemented in Cambridge sequential energy package (CASTEP) code [7]. Generalized gradient approximation (GGA) approach in the form of Perdew burke ernzerhof (PBE) is used to calculate the exchange and correlation functional [8]. The interactions between ionic cores and valence electrons are indicated by ultra-soft pseudo potentials. For Fe and P, the valence electrons considered are $3p^6 4s^2 3d^6$and $3s^2 3p^3$, respectively. A plane wave expansion method is applied for the optimization of the crystal structure. A special ***k***-point sampling in the first irreducible Brillouin zone is confirmed by Monkhorst-Pack scheme, and the ***k*** point mesh is selected as3×3×9, 9×9×12, 6×6×12, 6×12×6, 9×6×15, 6×3×3, 6×3×6 and 9×3×6 for Fe_3P, Fe_2P, o-FeP-1, o-FeP-2 (CoAs-structure and MnP-structure, simplified as o-FeP-1 and o-FeP-2), FeP_2, m-FeP_4-1, o-FeP_4 and m-FeP_4-2, respectively. A kinetic energy cut-off value of 400.0 eV is used for the plane wave expansion in reciprocal space. The selected ***k*** point is three times as much as the default values, and the cut-off energy has been tested. The result as shown in Fig. 1, the total energy will stay constant when the cut-off energy larger than 380eV for these compounds. So the selected values are suitable for the chosen system. The Broyden-Fletcher-Goldfarb-Shannon (BFGS)

method is applied to relax the whole structure based on total energy minimization. The total energy changes during the optimization processes are finally converged to 1×10^{-6} eV and the forces per atom are reduced to 0.05 eV / Å.

By using the stress-strain method according to the generalized Hooker's law, the elastic constants of the Fe_xP_y compounds are calculated. Several different strain modes are imposed on the crystal structure, and then the Cauchy stress tensor for each strain mode is estimated. Finally, the related elastic constants are identified as the coefficients in strain-stress relations as shown in Eq. (1) [9]

$$\begin{pmatrix}\sigma_1\\ \sigma_2\\ \sigma_3\\ \tau_4\\ \tau_5\\ \tau_6\end{pmatrix}=\begin{pmatrix}c_{11} & c_{12} & c_{13} & c_{14} & c_{15} & c_{16}\\ & c_{22} & c_{23} & c_{24} & c_{25} & c_{26}\\ & & c_{33} & c_{34} & c_{35} & c_{36}\\ & & & c_{44} & c_{45} & c_{46}\\ & & & & c_{55} & c_{56}\\ & & & & & c_{66}\end{pmatrix}\begin{pmatrix}\varepsilon_1\\ \varepsilon_2\\ \varepsilon_3\\ \gamma_4\\ \gamma_5\\ \gamma_6\end{pmatrix} \quad (1)$$

here, c_{ij} is the elastic constant, τ_i and σ_j are the shear stress and normal stress, respectively. The total number of independent elastic constants is determined by the symmetry of the crystal. For high symmetry point group, the required different strain patterns for the c_{ij} calculations can be greatly reduced. [9]

The cohesive energy and formation enthalpy are calculated to estimate the chemical stability of Fe_xP_y compounds. These two energy parameters are defined in Eqs. (2) and (3): [10]

$$E_{coh}(Fe_xP_y)=\frac{E_{tot}(Fe_xP_y)-xE_{iso}(Fe)-yE_{iso}(P)}{x+y} \quad (2)$$

$$\Delta_r H(Fe_xP_y)=\frac{E_{tot}(Fe_xP_y)-xE_{bin}(Fe)-yE_{bin}(P)}{x+y} \quad (3)$$

where $E_{coh}(Fe_xP_y)$ and $\Delta_r H(Fe_xP_y)$ are the cohesive energy and formation enthalpy of Fe_xP_y per

atom, respectively. $E_{tot}(Fe_xP_y)$ is the total energy of Fe_xP_y phase, E_{iso} is the total energy of a single Fe or P atom and E_{bin} refers to the cohesive energy of the Fe or P crystal, respectively. [10]

3. Results and discussions

3.1 Stability

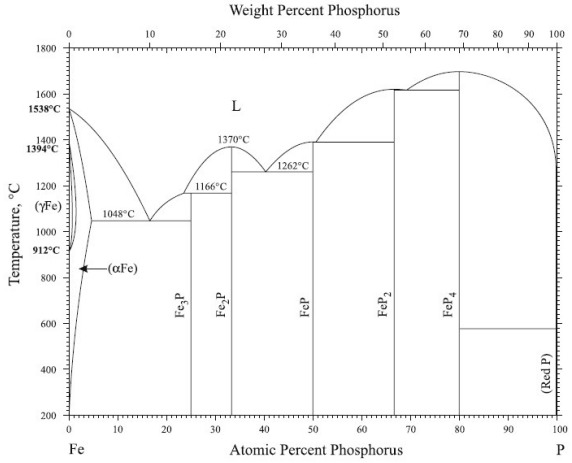

Fig. 2. The Fe-P equilibrium phase diagram

Fig. 2 shows the Fe-P equilibrium phase diagram [1] and the five Fe_xP_y binary phases are Fe_3P, Fe_2P, FeP, FeP_2, and FeP_4. With the increase of phosphorus content, the melting points of the Fe-P compounds increased. FeP_4 has the highest melting point as 1700℃ among the Fe-P compounds. The melting point of Fe_3P is the lowest may be ascribed to the weak covalent bonding between Fe atom and P atom. In fact, one example is Fe_3P as a common phase in grain-boundary segregation in some type steel material.

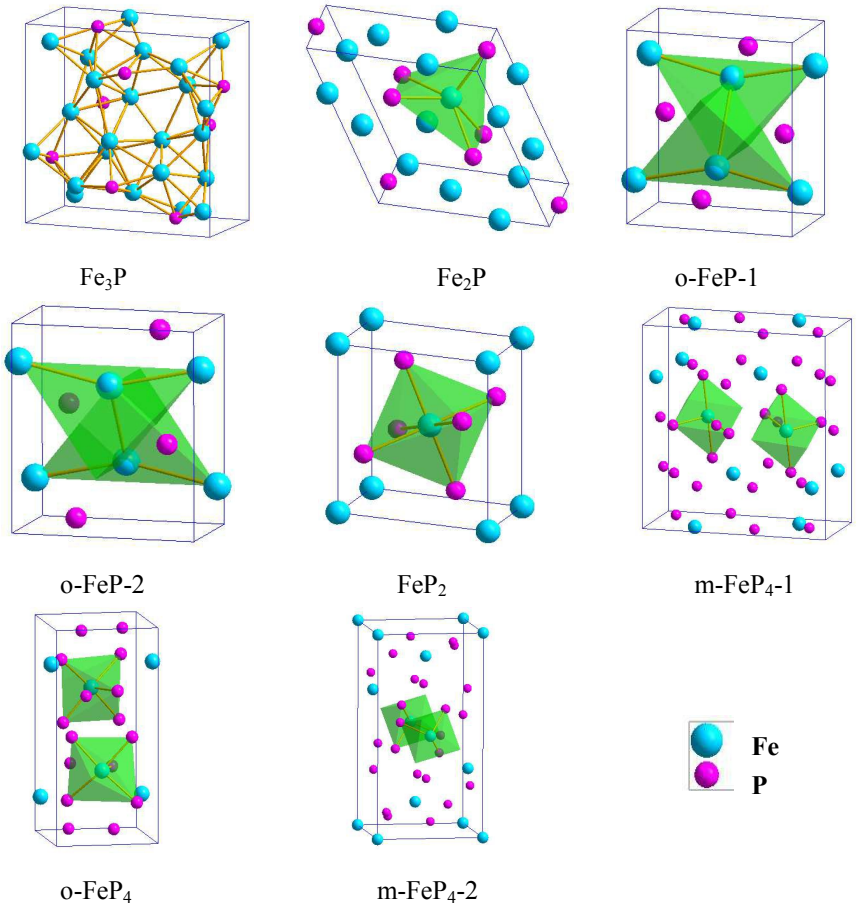

Fig. 3. The crystal structure of Fe-P compounds. The blue balls represent Fe atoms, the red balls refer to P atoms.

Fig. 3 shows the crystal structure of Fe-P compounds. The Fe_xP_y binary compounds contains four different types of crystal system, including tetragonal (Fe_3P), hexagonal (Fe_2P), orthorhombic (o-FeP-1, o-FeP-2, FeP_2, o-FeP_4), and monoclinic (m-FeP_4-1, m-FeP_4-2). The calculated lattice parameters of Fe, P and Fe-P compounds have been optimized, which are listed in Table 1. By compared these results, it can be seen that the calculated lattice parameters of o-FeP2 compounds are in good agreement with other calculated results and experimental values. [11-20] The average deviation of our result to experimental data for lattice parameters is less than 5.6%, which can be attributed to the approximation method in the work and thermodynamic effects on the crystal structures.

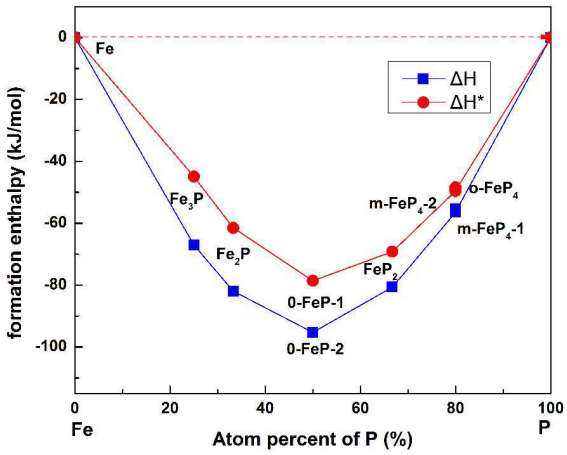

Fig. 4. The formation enthalpy (ΔH) and the spin-polarized formation enthalpy (ΔH*) of Fe-P binary compounds.

The cohesive energy and formation enthalpy are used to evaluate the stability of Fe-P binary compounds. As defined in Eqs. (2)-(3), the lower value for these two thermodynamic parameters, the more stable for the compound. The cohesive energy mainly reflects the stability of the combination with two atoms, while the formation enthalpy mainly reflects the stability of the formation of compounds. As shown in Table1, the calculated cohesive energy and formation enthalpy of studied Fe-P binary compounds are negative, which shows that Fe-P compounds are thermodynamically stable. The formation enthalpy without spin-polarized of Fe-P compounds are -67.068, -81.957, -78.580, -78.590, -69.200, -49.553, -48.395 and -49.370 kJ/mol, and the calculated spin-polarized formation enthalpy of Fe-P compounds are -44.950, -61.510, -78.580, -78.590, -69.200, -49.553, -48.395 and -49.370 kJ/mol for Fe_3P, Fe_2P, o-FeP_1, o-FeP_2, FeP_2, m-FeP_4_1, o-FeP_4, and m-FeP_4_2 phases, respectively. Fig. 4 shows the formation enthalpy (ΔH) and the calculated spin-polarized formation enthalpy (ΔH^*) curves as a function of P atom content for Fe-P binary compounds. Obviously, with the increase of phosphorus content, the formation enthalpy of Fe_xP_y compounds decrease at first and then increase. Which may due to the proportion of anti-bonding states decreasing at first and then increasing. For the ΔH, among all Fe-P binary

compounds, o-FeP_4 has the largest formation enthalpy value as -55.275 kJ/mol, and o-FeP_2 has the smallest formation enthalpy value as -95.255 kJ/mol. The stability sequence of eight Fe-P phase forms the following order: o-FeP_2 > o-FeP_1 > Fe_2P > FeP_2 > Fe_3P > m-FeP_4_1 > m-FeP_4_2 > o-FeP_4. For the ΔH^*, Fe_3P has the largest formation enthalpy value as -44.950 kJ/mol, and o-FeP_2 has the smallest formation enthalpy value as -78.590 kJ/mol. The stability sequence of these Fe-P phase forms the following order: o-FeP_2 > o-FeP_1 > FeP_2 > Fe_2P > m-FeP_4_1 > m-FeP_4_2 > o-FeP_4 > Fe_3P. Spin-polarization increased formation enthalpy of Fe_xP_y compounds, and the effect on the formation enthalpy weaken with the increased of phosphorus content. The stability sequence of the compounds changes with and without the spin-polarization. Form the result of the stability sequence it can be seen that the stability of Fe_3P and Fe_2P is reduced with the spin-polarization, which may due to the magnetic characters of Fe_3P and Fe_2P. According to the density of states, we can know that Fe_3P and Fe_2P have magnetic characters. In general, o-FeP_2 is the most stable compound among Fe-P compounds.

3.2 Elastic constants and polycrystalline moduli

The calculated elastic constants of the α-Fe, phosphorus and Fe-P compounds are listed in Table 2. The elastic stability conditions in various crystal systems can be expressed as [21,22]:

(1) orthorhombic (for o-FeP-1, o-FeP-2, FeP_2, o-FeP_4)：

$$c_{11}>0, c_{11}c_{22}>c_{12}^2, c_{11}c_{22}c_{33}+2c_{12}c_{13}c_{23}-c_{11}c_{23}^2-c_{22}c_{13}^2-c_{33}c_{12}^2>0, \\ c_{44}>0, c_{55}>0, c_{66}>0. \quad (4)$$

(2) tetragonal (for Fe_3P) and hexagonal (for Fe_2P)：

$$c_{11}>|c_{12}|, 2c_{13}^2<c_{33}(c_{11}+c_{12}), c_{44}>0, 2c_{16}^2<c_{66}(c_{11}-c_{12}). \quad (5)$$

(3) monoclinic (for m-FeP_4-1, m-FeP_4-2)：

$$c_{11}+c_{22}+c_{33}+2(c_{12}+c_{13}+c_{23})>0, c_{33}c_{55}-c_{35}^2>0, c_{44}c_{66}-c_{46}^2>0, c_{22}+c_{33}-2c_{23}>0,$$
$$c_{22}(c_{33}c_{55}-c_{35}^2)+2c_{23}c_{25}c_{35}-c_{23}^2c_{55}-c_{25}^2c_{33}>0,$$
$$2[c_{15}c_{25}(c_{33}c_{12}-c_{13}c_{23})+c_{15}c_{35}(c_{22}c_{13}-c_{12}c_{23})+c_{25}c_{35}(c_{11}c_{23}-c_{12}c_{13})]-[c_{15}^2(c_{22}c_{33}-c_{23}^2) \quad (6)$$
$$+c_{25}^2(c_{11}c_{33}-c_{13}^2)+c_{35}^2(c_{11}c_{22}-c_{12}^2)]+c_{55}g>0(g=c_{11}c_{22}c_{33}-c_{11}c_{23}^2-c_{22}c_{13}^2-c_{33}c_{12}^2$$
$$+2c_{12}c_{13}c_{23})>0, c_{ii}>0(i=1-6).$$

As shown in Table 2, the calculated elastic constants of each Fe-P compound satisfy the above criterion, which indicating that all of Fe-P compounds are mechanically stable. The calculated c_{11} and c_{22} of FeP_2 are larger than other elastic constants which indicates that they have high incompressible under uniaxial stress along crystallographic a (ε_{11}) and b (ε_{22}) axis. o-FeP_2 has the largest c_{33} value, which show that o-FeP_2 is very incompressible under uniaxial stress along crystallographic c (ε_{33}) axis. The largest elastic constant is the c_{22} of FeP_2 with 685.5 GPa. For two FeP polymorphs, the c_{22} of o-FeP_1 is close to the c_{33} of o-FeP_2 and the c_{33} of o-FeP_1 is close to the c_{22} of o-FeP_2, which indicates that in the terms of incompressible performance the b (ε_{22}) axis of o-FeP_1 is close to the c (ε_{33}) axis of o-FeP_2, and the c (ε_{33}) axis of o-FeP_1 is close to the b (ε_{22}) axis of o-FeP_1. c_{44}, c_{55} and c_{66} represents the shear modulus on (100), (010) and (001) crystal plane. From Table 2, one can see that Fe_2P has the largest c_{44} value and o-FeP_4 has the smallest c_{44} value for all Fe-P binary compounds. For three FeP_4 polymorphs, m-FeP_4_2 has the largest c_{44} value as 147.5 GPa.

The bulk modulus (B), shear modulus (G), Young's modulus (E) and Poisson's ratio (σ) of polycrystalline crystal are estimated with independent single crystal elastic constants according to the Viogt-Reuss-Hill (VGH) approximation [24]. The Voigt method is based on assumption of uniform strain throughout a polycrystal, which is given by:

$$9B_V=(c_{11}+c_{22}+c_{33})+2(c_{12}+c_{13}+c_{23}) \quad (7)$$

$$15G_V=(c_{11}+c_{22}+c_{33})-(c_{12}+c_{13}+c_{23})+3(c_{44}+c_{55}+c_{66}) \quad (8)$$

the Reuss method assumes a uniform stress and gives B and G as functions of the elastic compliance constants s_{ij}, which is the inverse matrix of c_{ij}.

$$1/B_R = (S_{11} + S_{22} + S_{33}) + 2(S_{12} + S_{13} + S_{23}) \quad (9)$$

$$1/G_R = 4[(S_{11} + S_{22} + S_{33}) - (S_{12} + S_{13} + S_{23})]/15 + (s_{44} + s_{55} + s_{66})/5 \quad (10)$$

the Voigt-Ruess-Hill (VRH) approximation is considered as a good estimated method for elastic modulus of polycrystalline.

$$G_H = (G_R + G_V)/2 \quad (11)$$

$$B_H = (B_R + B_V)/2 \quad (12)$$

the Young's modulus (E) and Poisson's radio (σ) can be calculated by follows: [25,26]

$$E = 9BG/(3B + G) \quad (13)$$

$$\sigma = (3B - 2G)/(6B + 2G) \quad (14)$$

The calculated bulk modulus (B), shear modulus (G), Young's modulus (E) and Poisson's ratio (σ) of these Fe-P binary compounds are shown in Table 4. Bulk modulus reveals the compressibility of the solid under hydrostatic pressure and the values are 315.8, 304.1, 235.5, 250.7, 284.2, 152.5, 153.6 and 147.7 GPa for Fe_3P, Fe_2P, o-FeP_1, o-FeP_2, FeP_2, m-FeP_4_1, o-FeP_4 and m-FeP_4_2, respectively. The bulk modulus values of Fe_3P and Fe_2P is higher than other carbides, such as Fe_3C (255 GPa) [28], TiC (242 GPa) [29] and Cr_3C (287.5 GPa) [30], but lower than h-WC (393.0 GPa) [31] and diamond (436.8 GPa) [32]. Fe_3P has the largest value of bulk modulus among Fe-P binary compounds, which may owe to its strongest ionic bond between Fe atom and P atom. Because the ionic bond have no direction. The calculated values of shear modulus are 84.0, 132.2, 148.7, 148.0, 176.8, 127.0, 129.4 and 125.4 GPa for Fe_3P, Fe_2P, o-FeP_1, o-FeP_2, FeP_2, m-FeP_4_1, o-FeP_4 and m-FeP_4_2, respectively. The largest value of shear modulus belongs to FeP_2, and the

largest value of Young's modulus is attributed to FeP_2. In addition, Fe_3P with the lowest P atom content has the largest bulk modulus as 315.8 GPa and the smallest shear modulus as 84.0 GPa. The result can be explained by the strong ionic bonding and weak covalent bonding of Fe_3P, because the ionic bond have no direction, covalent bond has directionality.

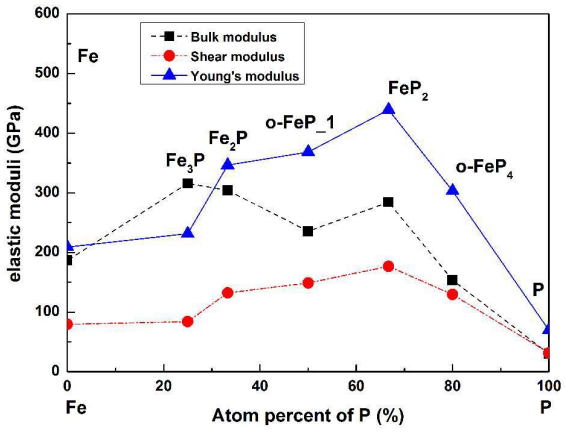

Fig. 5. Polycrystalline elastic moduli of Fe-P binary compounds.

Fig. 5 presents the bulk modulus, shear modulus and Young's modulus curves as a function of P atom content for Fe-P system. With the increase of phosphorus content, the three moduli of the Fe-P compounds first decrease again increase to decrease again. The ratio of B/G (here B_H and G_H are used) can be used to indicate the ductile or brittle of the compounds, a high value is associated with ductility and a low value is associated with brittleness, the critical value is about 1.75. Fig. 6 shows the B/G and Poisson's ratio curves as a function of P atom content for Fe-P system. When comparing the B/G value, it's clearly imply that Fe_3P and Fe_2P are considered to be ductile compound since the value of B/G is larger than 1.75, m-FeP_4-2 has the smallest value as 1.18, indicating it's the most brittle. The result is in good agreement with the analysis of density of states. Meanwhile, the Poisson's ratio larger or smaller than 0.25 can also be used to indicate the ductile or brittle of the compounds. From Fig. 6, we can know that Fe_3P and Fe_2P can be classified as ductility,

which may owe to the strong metallic bonding in it. While three FeP_4 compounds, two FeP compounds and FeP_2 should be classified as brittleness, since the value of B/G is smaller than 1.75 and the value of Poisson's ratio is smaller than 0.25. This may owe to the strong covalent bonding in it.

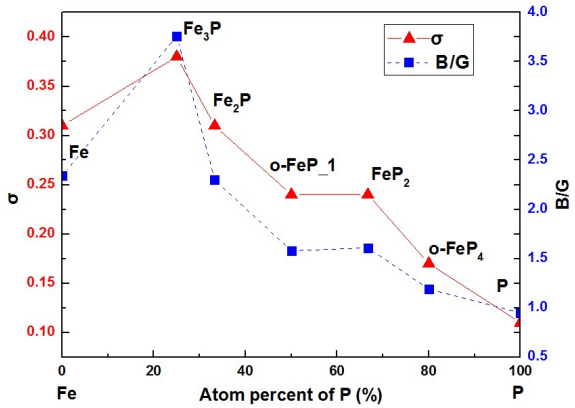

Fig. 6. The B/G and σ values of the Fe-P binary compounds.

The hardness (H_v) is very important in the applications of Fe-P binary compounds. In the present paper, the hardness of two FeP compounds is estimated by a relatively semi-empirical equation [33,44]. The equation is defined as following:

$$H_v = AN_a e^{-\alpha f_i} E_h,$$
$$N_a = \left(\sum_i n_i Z_i \Big/ 2v \right)^{2/3}, f_i = 1 - \exp\left[-(x_A - x_B)^2 \Big/ 4 \right], E_h = 39.74 \Big/ d^{2.5} \quad (15)$$

where H_v denotes the hardness, A is a proportional coefficient, α is a constant. A=14, α =-1.191. n_i is the number of i atom in the cell, Z_i is the valence electron number of i atom, v is the cell volume. x_A is the electronegativities of A atom, d is the bond length in angstroms. The calculated hardness of FeP compounds are shown in Table 3.

3.3 Anisotropy of elastic properties

The mechanical anisotropy is important in the applications of Fe-P materials. The fracturing

crack of materials forms not only in the substrate, but also in the inclusion. The formation and propagation of micro cracks is often related to the elastic anisotropy. Knowing the anisotropy of Fe_xP_y compounds would be helpful to design and enhance some special device. To describe the degrees of anisotropy of Fe-P binary compounds, a numbers of indexes, including the shear anisotropic factors (A_1, A_2 and A_3), the percentages of anisotropy in the compression and shear (A_B and A_G) and a universal elastic anisotropy index (A^U) are calculated by the following equations [34,35,36].

$$A_1 = \frac{4C_{44}}{C_{11}+C_{33}-2C_{13}} \quad \text{for (100) plane} \tag{16}$$

$$A_2 = \frac{4C_{55}}{C_{22}+C_{33}-2C_{23}} \quad \text{for (010) plane} \tag{17}$$

$$A_3 = \frac{4C_{66}}{C_{11}+C_{22}-2C_{12}} \quad \text{for (001) plane} \tag{18}$$

$$A_B = \frac{B_V - B_R}{B_V + B_R} \times 100 \tag{19}$$

$$A_G = \frac{G_V - G_R}{G_V + G_R} \times 100 \tag{20}$$

$$A^U = 5\frac{G_V}{G_R} + \frac{B_V}{B_R} - 6 \geq 0 \tag{21}$$

where B_V, B_R, G_V and G_R are the bulk and shear modulus calculated with Voigt and Reuss methods, respectively. The calculated results are shown in Table 4. For A_1, A_2 and A_3, a value of unity imply isotropic and a non-unity value imply anisotropic for a crystal. For isotropic structures, the values of A_B, A_G and A^U are zero. Meanwhile the large discrepancies from zero indicate the highly mechanical anisotropic properties.

From Table 4, it can be seen that Fe is isotropic, Fe_2P and m-FeP_4.2 have strong isotropy, and Fe_3P has the strongest anisotropy especially in (001) plane. Fe_3P has the largest value of A_G as 22.43% among all Fe-P binary compounds, implying that the anisotropy in shear modulus for Fe_3P

is the strongest. However, the A_1, A_2, A_3, A_B and A_G can't fully describe the elastic anisotropy. The A_1, A_2 and A_3 describe the anisotropy of the shear modulus in different crystal plane, the index A^U is considered as an appropriate parameter to describe the degrees of elastic anisotropy of the compound. From the Table 4, Fe_3P has the strongest anisotropy of the Fe-P binary compounds, since the value of A^U is 2.89, and m-FeP_4.2 has the strongest isotropy among the Fe_xP_y compounds, since the value of A^U is 0.35.

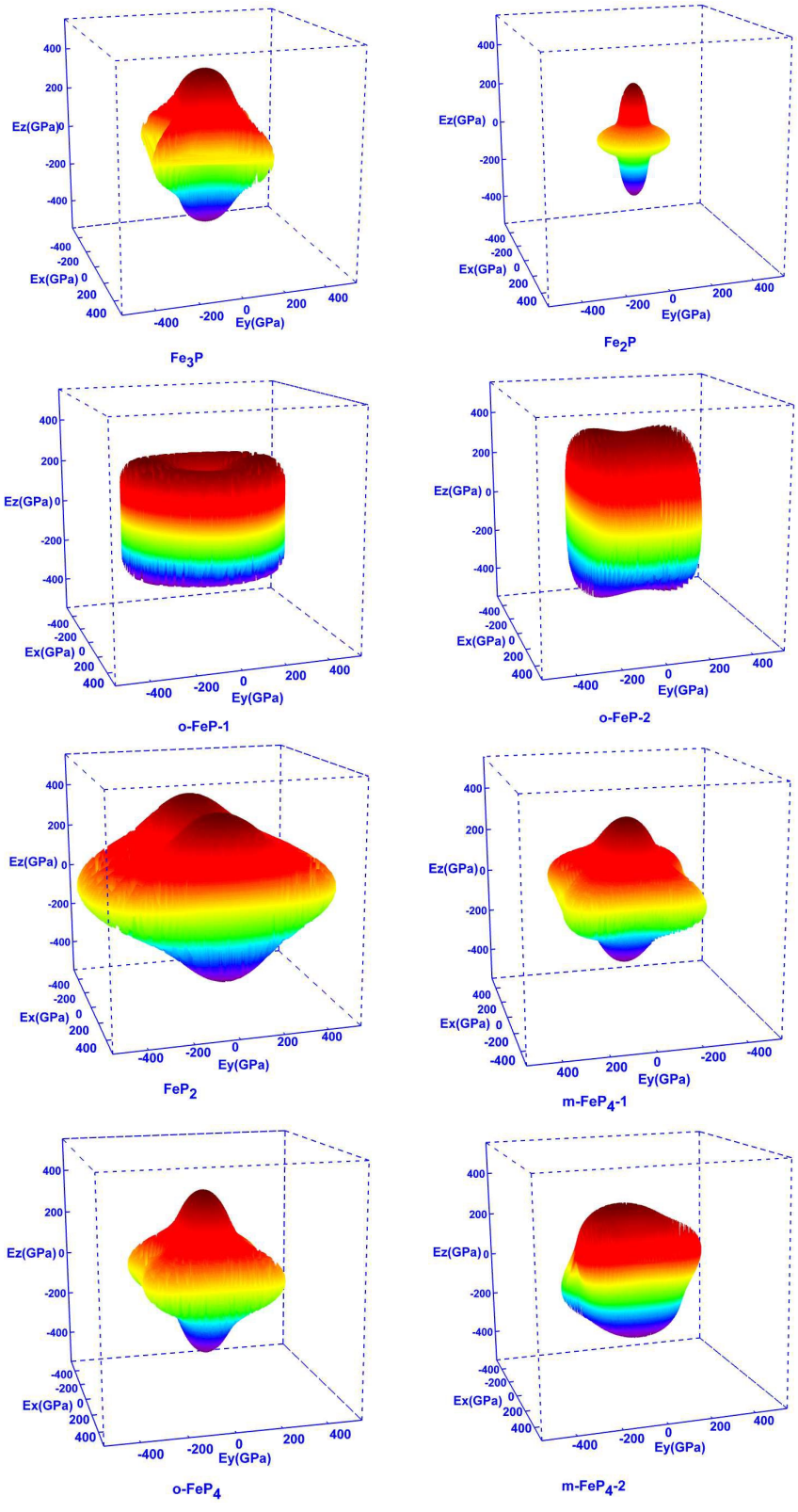

Fig. 7. Contour plots of Young's modulus of Fe-P compounds in 3-D space.

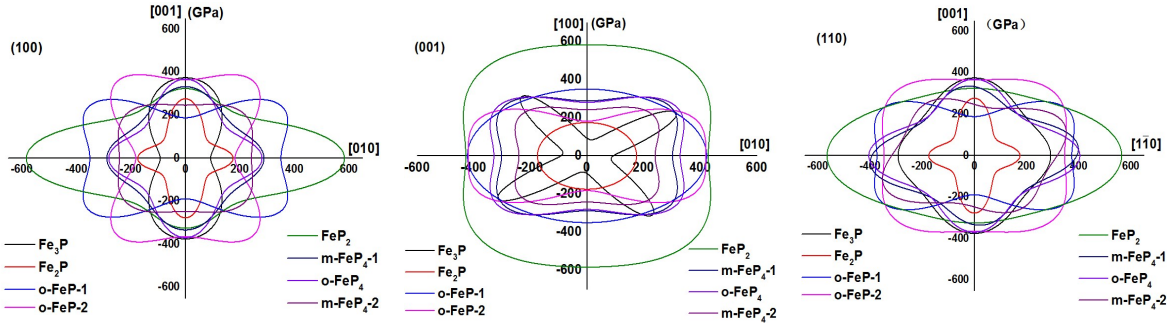

Fig. 8. Planar projections of Young's modulus of Fe-P compounds at (100), (001) and(110) crystallographic planes.

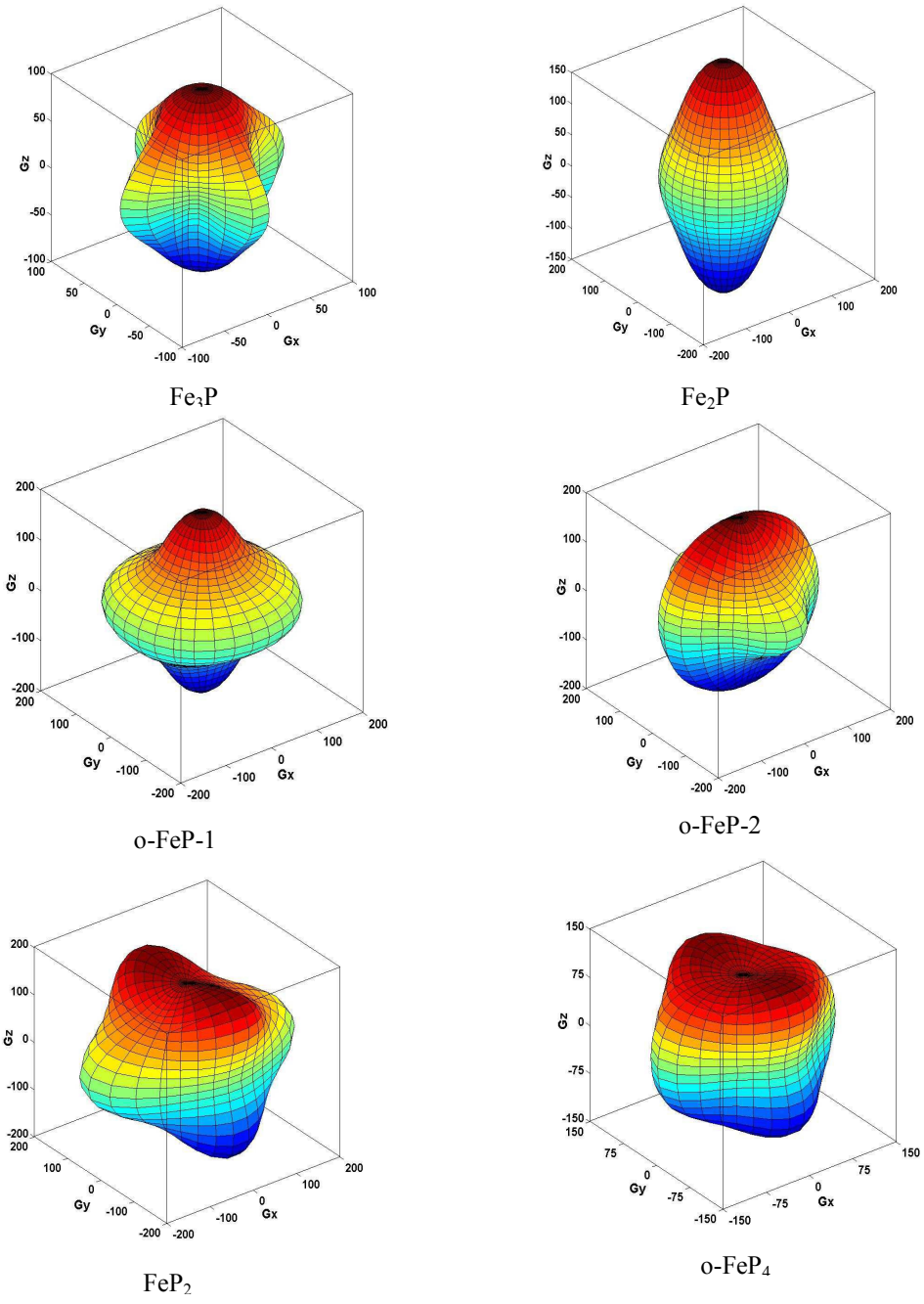

Fig. 9. Contour plots of shear modulus (GPa) of Fe-P compounds in 3-D space.

The most straightforward way to illustrate the elastic anisotropy is to plot the Young's modulus and shear modulus in three dimensions (3D) as a function of the crystallographic direction. The directional dependence of Young's modulus and shear modulus is given by [10,34,37,38,42, 43]:

Hexagonal crystal (for Fe_2P)

$$\frac{1}{E} = (1-l_3^2)^2 s_{11} + l_3^4 s_{33} + l_3^2(1-l_3^2)(2s_{13}+s_{44}) \quad (22)$$

$$\frac{1}{G} = S_{44} + \left[\left(S_{11}-S_{12}\right) - \frac{1}{2}S_{44} \right]\left(1-l_3^2\right) + 2\left(S_{11}+S_{33}-2S_{13}-S_{44}\right) l_3^2\left(1-l_3^2\right)$$

Orthorhombic crystal (for o-FeP_1, o-FeP_2, FeP_2, o-FeP_4)

$$\frac{1}{E} = s_{11}l_1^4 + s_{22}l_2^4 + s_{33}l_3^4 + (2s_{12}+s_{66})l_1^2l_2^2 + (2s_{13}+s_{55})l_1^2l_3^2 + (2s_{23}+s_{44})l_2^2l_3^2 \quad (23)$$

$$\frac{1}{G} = 2S_{11}l_1^2\left(1-l_1^2\right) + 2S_{22}l_2^2\left(1-l_2^2\right) + 2S_{33}l_3^2\left(1-l_3^2\right) - 4S_{12}l_1^2l_2^2 - 4S_{13}l_1^2l_3^2 - 4S_{23}l_2^2l_3^2$$
$$+\frac{1}{2}S_{44}\left(1-l_1^2-4l_2^2l_3^2\right) + \frac{1}{2}S_{55}\left(1-l_2^2-4l_1^2l_3^2\right) + \frac{1}{2}S_{66}\left(1-l_3^2-4l_1^2l_2^2\right)$$

Monoclinic crystal (for m-FeP_4_1, m-FeP_4_2)

$$\frac{1}{E} = l_1^4 s_{11} + l_2^4 s_{22} + l_3^4 s_{33} + 2l_1^2l_2^2 s_{12} + 2l_1^2l_3^2 s_{13} + 2l_1^3l_2 s_{15} + 2l_2^2l_3^2 s_{23} + 2l_1l_2^2l_3 s_{25} + l_2^2l_3^2 s_{44} \quad (24)$$
$$+2l_1l_2^2l_3 s_{46} + l_1^2l_3^2 s_{55} + l_1^2l_2^3 s_{66}^6$$

Tetragonal (for Fe_3P)

$$\frac{1}{E} = s_{11}(1-l_3^2)^2 + s_{33}l_3^4 + (2s_{13}+s_{44})l_3^2(1-l_3^2) \quad (25)$$

$$\frac{1}{G} = 2S_{11}l_1^2\left(1-l_1^2\right) + 2S_{22}l_2^2\left(1-l_2^2\right) + 2S_{33}l_3^2\left(1-l_3^2\right) - 4S_{12}l_1^2l_2^2 - 4S_{13}l_1^2l_3^2 - 4S_{23}l_2^2l_3^2$$
$$+\frac{1}{2}S_{44}\left(1-l_1^2-4l_2^2l_3^2\right) + \frac{1}{2}S_{55}\left(1-l_2^2-4l_1^2l_3^2\right) + \frac{1}{2}S_{66}\left(1-l_3^2-4l_1^2l_2^2\right)$$

where s_{ij} are the elastic compliance constants, and l_1, l_2 and l_3 are the directional cosines. The surface contours of the Young's modulus and shear modulus of Fe-P binary compounds are illustrated in Fig. 7 and Fig. 9. For an isotropic system, the graph would be a sphere. Obviously, Fe_3P, Fe_2P, FeP_2, m-FeP_4_1 and o-FeP_4 show a strong anisotropic character in Young's modulus, and Fe_3P, two FeP compounds, FeP_2 and o-FeP_4 show a strong anisotropic character in shear modulus. The surface contour of two FeP compounds and m-FeP_4_2 in Fig.7 is close to an cylinder, which means that the Young's modulus of these compounds have weaker anisotropy than other

compounds. Projections of the Young's modulus on the (100), (001) and (110) planes shows more details about the anisotropic properties of Young's modulus as shown in Fig. 8. Obviously, Young's modulus has a strong directional dependence on these planes. From Fig. 8, we can see that FeP_2 shows the maximum Young's modulus along the [010] and [110] direction, and Fe_3P shows the minimum Young's modulus along the [010] direction one the (100) and (001) plane. For Fe_2P, the planar contours on the (001) planes is close to an ellipse, which means that the Young's modulus of Fe_2P on the (001) planes has weaker anisotropy than other compounds.

3.4 Electronic structures

The electronic structures and chemical bonding characteristics of Fe_xP_y compounds are indicated by the electron density distribution map, total density of states (TDOS) and partial density of states (PDOS).

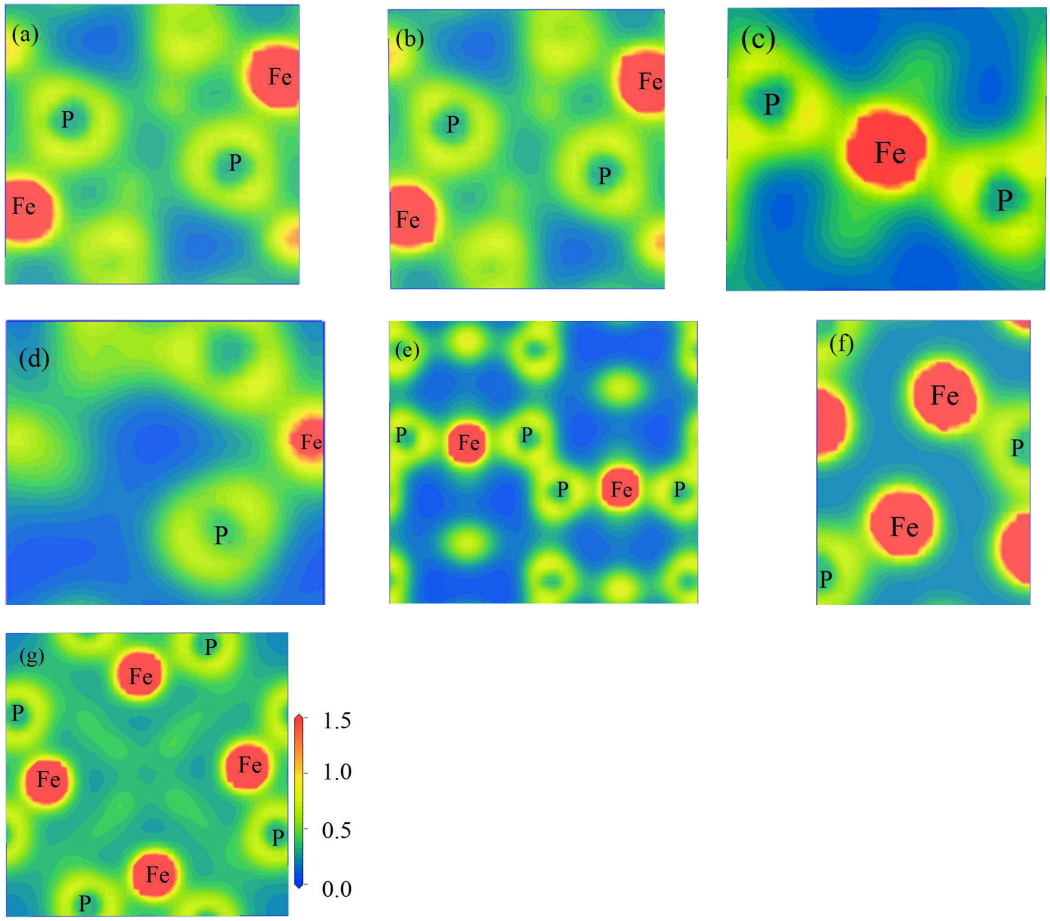

Fig. 10. Total electron density distribution through (-0.563 0.318 0.763), (0.561 -0.764 -0.318), (-0.021 -0.020 0.999), (-0.039 -0.355 -0.934), (1 0 0), (0 0 1) and (-0.012 -0.012 0.999) slice intersecting both Fe and P atoms for (a) o-FeP-1, (b) o-FeP-2, (c) FeP_2, (d) o-FeP_4, (e) m-FeP_4-1, (f) Fe_2P and (g) Fe_3P compounds, respectively.

The calculated total electron density distribution maps of Fe-P compounds are shown in Fig. 10. Electronic mainly concentrated on the iron atoms. For o-FeP-1, o-FeP-2, Fe2P and Fe3P, the electron density values are large than zero even in the interstitial regions, which indicate the metallic nature of these compounds. The elongated contours along Fe-P bond axis show the covalent interaction. m-FeP4-1 has the strongest covalent bonding between P and P.

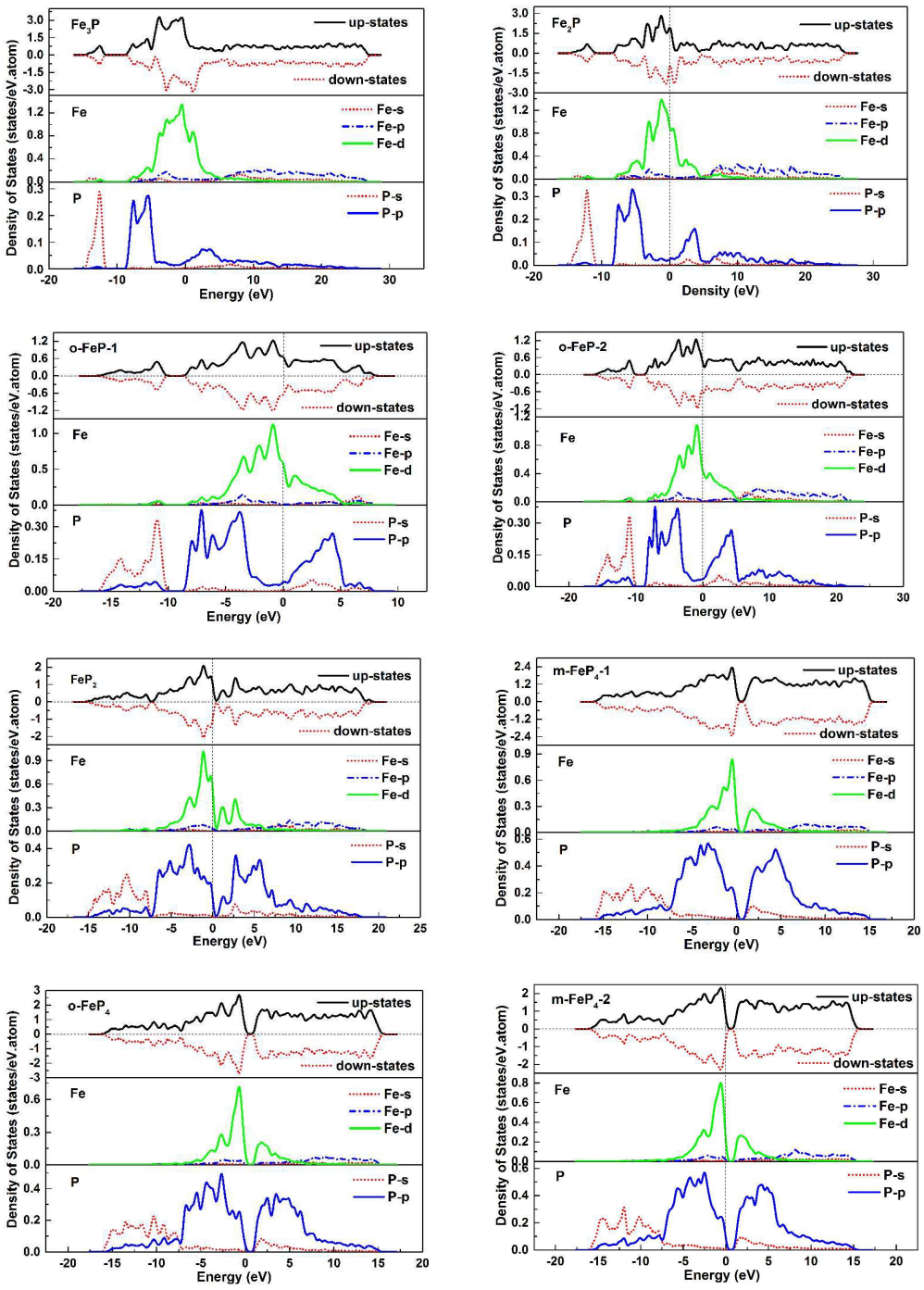

Fig. 11. The total density of states (TDOS) and partial density of states (PDOS) for Fe_xP_y compounds, dashed lines represent the Fermi level.

The TDOS and PDOS of Fe_xP_y compounds are shown in Fig. 11. The nature of magnetic characters can be understood from the spin-polarized total density of states. Comparing the up with

down densities, it can be seen that the up and down states are not symmetric for Fe_3P and Fe_2P, which indicates they have magnetic characters. Actually, the low and high valence band is almost symmetric, and it is near to the Fermi level that the up and down states are dissymmetric. While for other compounds, the up and down states are symmetric, so they have no magnetic characters. No energy gap near to the Fermi level can be seen for Fe_3P, Fe_2P, o-FeP_1 and o-FeP_2, which indicates the metallicity and electronic conductivity of these binary compounds. Based on the analysis of band structure, the energy gap near to the Fermi level for FeP_2, o-FeP_4, m-FeP_4-1 and m-FeP_4-2 are 0.573, 0.903, 0.924 and 1.16 eV, respectively. So these four compounds are considered to be semiconductor, and the electroconductibility of m-FeP_4-2 is the worst. Other compounds belong to conductor. We can see that the TDOS values in Fermi levels increased as the Fe atom content increased. The Fe_3P has the strongest metallicity, which is consistent with the opinion of B/G and Poisson's ratio (σ).The Fe-d bands of m-FeP_4-1 have a peak, which shows that the electron of d bands is relatively local state. From the Fig. 11, it can be seen that the ground state properties of Fe-P binary compounds are determined by 3d bands of Fe. At the low energy part, the band from -9 eV to -5 eV is mainly contributed by 3p bands of P. The Fe-d bands are overlapped with the P-p bands in the energy range from -4 eV to 3 eV for three FeP_4 compounds, which indicates the covalent interactions because of the strong hybridization between Fe-d bands and P-p bands. It's similar with the energy range from -2 eV to 3 eV of FeP_2. The Fe-d band hybridizes weakly with the P-p in the energy range from -5 eV to -2 eV for o-FeP_1 and o-FeP_2. We can see that the FeP_4 compounds have the strongest covalent interaction among all Fe_xP_y compounds from Fig. 11, which lends to the highest melting point. This result is in consistent with the Fe-P equilibrium phase diagram. The valence electrons of Fe and P atom considered are $3p^6 3d^6 4s^2$ and $3s^2 3p^3$. For Fe_3P, the

position of Fe-d bands does not coincide with the P-p bands, which shows the interaction between the electrons of P and Fe atom. The Fe 3d orbitals loses an electron and forms the partially fulled state, the P 3p orbitals gets three electrons and forms the entirely fulled state. In addition, the partially fulled and entirely fulled states are stable state. The electron transfer path implies ionic interaction in Fe_3P compounds. In a word, with the increase of phosphorus content, the covalent interaction of the Fe-P binary compounds strengthens, and the ionic interaction and metallicity weakens.

According to above discussions, Fe_3P and Fe_2P have magnetic characters. m-FeP_4-2 is considered to be semiconductor. The bonding behaviors of Fe-P binary compounds are the combinations of metallic, covalent and ionic bonds. For Fe_3P and Fe_2P, the chemical bonding is dominated by the Fe-P ionic bonds. The chemical bonding of o-FeP_1, o-FeP_2, FeP_2, m-FeP_4_1, o-FeP_4 and m-FeP_4_2 is dominated by the Fe-P covalent bonds but also possesses the ionic and metallic character, which may lead to the high melting point.

3.5 Debye temperature

It is certain that the sound velocity and Debye temperature can be used to evaluate the chemical bonding characteristics and thermal properties of compounds. The sound velocity and Debye temperature at the low-temperature are calculated with the previously obtained bulk modulus (B) and shear modulus (G). The Debye temperature can be calculated by the following equation: [39,9]

$$\Theta_D = \frac{h}{k_B}\left[\frac{3n}{4\pi}\left(\frac{N_A\rho}{M}\right)\right]^{1/3} \nu_m \quad (26)$$

where, Θ_D represents Debye temperature; h and k_B is Plank and Boltzmann constant, respectively; n is the total number of atoms per formula; N_A is the Avogadro constant; M is the molecular weight

per formula; ρ is the theoretical density, and the v_m is the average sound velocity defined as:

$$v_m = \left[\frac{1}{3}\left(\frac{2}{v_s^3}+\frac{1}{v_t^3}\right)\right]^{-1/3} \quad (27)$$

$$v_s = \sqrt{G/\rho} \quad (28)$$

$$v_t = \sqrt{\left(B+\frac{4}{3}G\right)\frac{1}{\rho}} \quad (29)$$

where, v_s is the transverse sound velocity and v_l is the longitudinal sound velocity; B and G are isothermal bulk modulus and shear modulus. [22,40,41] .

The value of Debye temperature and sound velocities of Fe-P binary compounds are listed in Table 5. Debye temperature reflects the strength of chemical bonding in crystal structure. From the Table 5, we can see that the Debye temperature increases with P atom content increases in the Fe-P binary compounds expect for FeP_2. Moreover, Fe_3P has the lowest Debye temperature and highest B/G ratio, which indicates the strongest metallic character. It is consistent with the previous calculations on the density of states. Besides, the average sound velocities of these Fe_xP_y compounds are relatively large about 5500 m/s except Fe_3P. A reasonable explanation is these compounds with high bulk and shear modulus and low density, the v_l and v_s are correlated to bulk modulus, shear modulus and density.

4. Conclusions

In general, we have investigated stability, mechanical properties and electronic structures of all Fe-P binary compounds with first-principles calculations. The cohesive energy and formation enthalpy indicate that they are thermodynamically stable. The elastic constants of the Fe_xP_y compounds satisfy the mechanical stability criterions. Fe_3P has the largest bulk modulus as 315.8 GPa and the smallest shear modulus as 84.0 GPa. FeP_2 exhibits the largest shear and Young's

modulus as 176.8 and 439.3 GPa, respectively. The hardness of two FeP compounds is 33.39 GPa. Fe_3P and Fe_2P are considered to be ductile compound, which may own to the strong metallic bonding in it, The 3D surface contour of Young's modulus and shear modulus is plotted to verify the mechanical anisotropy of Fe-P binary compounds, Fe_3P has the strongest anisotropy among the Fe_xP_y compounds. The bonding behaviors of Fe-P binary compounds are the combinations of metallic, covalent and ionic bonds. Fe3P and FeP2 have the smallest and largest Debye temperature as 497.1 K and 822.4 K, respectively.

Acknowledgments

This work was supported by the National Natural Science Foundation of China (Nos.51171074 and 51261013).

References

[1] Ohtani H, Hanaya N, Hasebe M, Teraoka S, Abe M, Calphad, 2006, 30, 147-58.

[2] Zhou W, Liu L-J, Li B-L, Wu P, Song Q-G, Comput Mater Sci, 2009, 46, 921-31.

[3] Hohenberg P, Kohn W, Phys Rev B, 1964, 136, 864.

[4] Li J-Y, Chen H-M, Gao Q-Z, Xie Q-L, Huang J-L, Journal of Guangxi University, Nat Sci Ed, 2009, 34, 565-70.

[5] Chen L, Kurita N, Fujiwara T, Abliz M, Hedo M, Oguro, Matsuo A, Kindo K, Uwatoko, Fujii H, Journal of Magnetism and Magnetic Materials, 2007, 310, 219-21.

[6] Tobola J, Bacmann M, Fruchart D, Kaprzyk S, Koumina A, Niziol S, Soubeyroux J L, Wolfers P, Zach R, Journal of Magnetism and Magnetic Materials, 1996, 157-158, 708-10.

[7] Liu H-L, Wang W-L, Hu L, Wei B-B, Intermetallics, 2014, 46, 211-21.

[8] Perdew J P, Burke K, Ernzerhof M, Phys Rev Lett, 1996, 77, 3865.

[9] Feng J, Xiao B, Chen J, Du Y, Yu J, Zhou R, Mater Des, 2011, 32, 3231-39.

[10] Chong X-Y, Jiang Y-H, Zhou R, Feng J, J Alloys Compd, 2014, 610, 684-94.

[11] Haglund J, Fernandez Guillermet A, Grimvall G, Korling M, Phys Rev B, 1993, 48, 11685-91.

[12] Rundqvist S, Acta Chemical Scandinavica, 1962, 16, 1-19.

[13] Koumina A, Bacmann M, Fruchart D, Soubeyroux J L, Wolfers P, Tobola J, Kaprzyk S, Niziol S, Mesnaoui M, Zach R, Annales de Chimie Science des Materiaux, 1998, 23, 177-80.

[14] Selte K, Kjekshus A, Acta Chemical Scandinavica, 1972, 26, 1276-77.

[15] Rundqvist S, Nawapong P C, Acta Chemical Scandinavica, 1965, 19, 1006-8.

[16] Dahl E, Acta Chemical Scandinavica, 1969, 23, 2677-84.

[17] Evain M, Brec R, Fiechter S, Tributsch H, Journal of Solid State Chemistry, 1987, 71, 40-6.

[18] Sugitani M, Kinomura N, Koizumi M, Kume S, Journal of Solid State Chemistry, 1978, 26, 195-201.

[19] Jeitschko W, Braun D J, Acta Csystallographica Section B, 1978, 34, 3196-201.

[20] Ahuja R, Physical Status Solidi Sectio B, 2003, 235, 282-7.

[21] Felix Mouhat, Coudert F X, Phys Rev B, 2014, 90, 224104.

[22] Chong X-Y, Jiang Y-H, Zhou R, Feng J, Comput Mater Sci, 2014, 87, 19-25.

[23] Shang S-L, Saengdeejing A, Mei Z-G, Kim D E, Zhang H, Ganeshan S, et al, Comp Mater Sci, 2010, 48, 813-26.

[24] Zhou W, Liu L, Li B, Wu P, Song Q, Comput Mater Sci, 2009, 46, 921.

[25] Hill R, Proc Phys Soc Lond Sect A, 1952, 65, 349-54.

[26] Xiao B, Feng J, Zhou C T, Jiang Y H, Zhou R, J Appl Phys, 2011, 109, 023507-9.

[27] Frechen T, Dietz G. J Phys F, Met Phys, 1984, 14, 1811-26.

[28] Zhou C T, Xiao B, Feng J, Xing J D, Xie X J, Chen Y H, Zhou R, Comput Mater Sci, 2009, 45, 986.

[29] Gilman J J, Roberts B W, J Appl Phys, 1961, 32, 1405.

[30] Li Y F, Gao Y M, Xiao B, Min T, Yang Y, Ma S Q, Yi D W, J Alloys Compd, 2011, 509, 5242-9.

[31] Li Y F, Gao Y M, Xiao B, Min T, Fan Z J, Ma S Q, Xu L L, J Alloys Compd, 2010, 502, 28-37.

[32] Liang Y C, Guo W L, Fang Z, Acta Phys Sin, 2007, 56, 4847.

[33] Gao F M, He J L, Wu E D, Liu S M, Yu D L, L i D C, Zhang S Y, Tian Y J, Phys Rev Lett, 2003, 91, 015502.

[34] Panda K B, Ravi Chandran K S, Acta Mater, 2006, 54, 1641-57.

[35] Chen X Q, Niu H Y, Li D Z, Li Y Y, Intermetallics, 2011, 19, 1275-81.

[36] Miao N H, Sa B S, Zhou J, Sun Z M, Comput Mater Sci, 2011, 50, 1559-66.

[37] Ding A L, Li C M, Wang J, Ao J, Li F and Chen Z Q, Chin Phys B, 2014, 23, 096201.

[38] Feng J, Xiao B, Zhou R, Pan W, Acta Mater, 2013, 61, 7364-83.

[39] Feng J, Xiao B, Zhou R, Pan W, D.R. Clarke, Acta Mater, 2012, 60, 3380-92.

[40] Liu Y Z, Jiang Y H, Zhou R, Feng J, J Alloys Compd, 2014, 582, 500.

[41] Feng J, Xiao B, Wan C L, Qu Z X, Huang Z C, Chen J C, Zhou R, Pan W, Acta Mater, 2011, 59, 1742-60.

[42] Cheng X Y, Chen X Q, Li D Z, Li Y Y, Acta Crystallogr, 2014, 70, 85-103.

[43] Chen Z Q, Wang J, Li C M, Journal of Alloys and Compounds, 2013, 575, 137-144.

[44] Phillips J C, Rev Mod Phys, 1970, 42, 320.

Table 1 The space group, calculated lattice parameters, V_{cell}, cohesive energy (kJ/mol), formation enthalpy Δ_rH (kJ/mol) and the calculated spin-polarized formation enthalpy Δ_rH^* (kJ/mol) of Fe-P binary compounds.

Substances	space group	Composition at %P	a(Å)	b(Å)	c(Å)	V_{cell}(Å^3)	E_{coh}	Δ_rH	Δ_rH^*
Fe	Im-3m	0	3.402	3.402	3.402	39.369	-898.415	0	0
			3.430[a]	3.430[a]	3.430[a]	40.350[a]			
Fe_3P	I-4	25.000	8.598	8.598	4.277	316.109	-848.235	-67.068	-44.950
			9.107[b]	9.107[b]	4.460[b]	369.900[b]			
Fe_2P	P-62m	33.333	5.531	5.531	3.399	90.062	-834.725	-81.957	-61.510
			5.690[c]	5.690[c]	3.458[c]	96.960[c]			
			5.704[d]	5.704[d]	3.431[d]				
o-FeP_1	Pna21	50.000	5.055	5.680	2.931	84.146	-791.300	-95.236	-78.580
			5.193[e]	5.792[e]	3.099[e]	93.210[e]			
o-FeP_2	Pnma	50.000	5.053	2.932	5.680	84.152	-791.300	-95.255	-78.590
			5.191[f]	3.099[f]	5.792[f]	93.180[f]			
FeP_2	Pnnm	66.700	4.883	5.536	2.647	71.560	-720.855	-80.674	-69.200
			4.973[g]	5.657[g]	2.723[g]	76.600[g]			
m-FeP_4_1	C12/c1	80.000	4.968	10.261	10.939	557.632	-651.375	-56.443	-49.553
			5.054[h]	10.407[h]	11.069[h]	582.120[h]			
o-FeP_4	C2221	80.000	4.923	10.077	5.434	269.551	-649.445	-55.275	-48.395
			5.005[i]	10.213[i]	5.530[i]	282.670[i]			
m-FeP_4_2	P121/c1	80.000	4.540	13.444	6.914	413.839	-650.410	-56.260	-49.370
			4.619[j]	13.670[j]	7.002[j]	433.270[j]			
P	Cmca	100.000	3.289	10.832	4.390	156.408	-526.890	0	0
			3.241[k]	10.192[k]	4.239[k]	140.000[k]			

a Cal. in Ref. [11]

b Exp. in Ref. [12]

c Exp. in Ref. [13]

d Cal. in Ref. [4]

e Exp. in Ref. [14]

f Exp. in Ref. [15]

g Exp. in Ref. [16]

h Exp. in Ref. [17]

i Exp. in Ref. [18]

j Exp. in Ref. [19]

k Cal. in Ref. [20]

Table 2 Single crystalline elastic constants (c_{ij}, in GPa) of Fe-P binary compounds.

Substances	Fe	Fe_3P	Fe_2P	o-FeP_1	o-FeP_2	FeP_2	m-FeP_4_1	o-FeP_4	m-FeP_4_2	P
c_{11}	266.4[a]	418.2	460.3	502.5	506.4	570.0	335.9	367.5	279.9	188.4
	279.2[b]									
c_{22}		418.2	460.3	476.4	280.1	685.5	325.2	310.8	285.6	42.9
c_{33}		513.5	474.7	277.4	529.9	382.4	344.2	374.3	285.5	39.3
c_{44}	96.3[a]	98.1	183.9	176.5	171.3	105.9	91.6	76.7	147.5	19.9
	93.0[b]									
c_{55}		98.1	183.9	177.1	170.0	228.4	109.3	121.1	136.8	55.0
c_{66}		136.6	88.9	165.6	176.6	227.1	188.3	189.2	160.0	31.9
c_{12}	146.5[a]	348.4	282.4	136.9	147.6	239.0	99.5	104.0	90.4	-1.2
	148.8[b]									
c_{13}		230.6	195.7	144.5	166.7	180.5	41.1	44.0	73.2	36.0
			172.0[c]							
c_{15}							-7.3		16.6	
c_{23}		230.6	195.7	183.8	210.0	97.2	44.1	20.9	75.7	2.5
c_{25}							18.5		21.8	
c_{35}							-15.9		-26.5	
c_{46}							17.7		26.1	

a Cal. in Ref. [7]

b Cal. in Ref. [23]

c Cal. in Ref. [4]

Table 3 Polycrystalline elastic properties of Fe-P binary compounds, including Bulk modulus (B), Shear modulus (G), Young's modulus (E), Poisson's ratio (σ) and Vickers hardness (H_v).

Substances	Fe	Fe_3P	Fe_2P	o-FeP_1	o-FeP_2	FeP_2	m-FeP_4_1	o-FeP_4	m-FeP_4_2	P
B_V(GPa)	186.5[a]	315.8	304.8	243.0	262.8	296.8	152.7	154.5	147.7	38.4
B_R(GPa)	186.5[a]	315.7	303.5	228.1	238.7	271.7	152.3	152.7	147.6	21.7
B_H(GPa)	186.5[a]	315.8	304.1	235.5	250.7	284.2	152.5	153.6	147.7	30.0
G_V(GPa)	81.7[a]	102.6	139.5	156.6	156.4	187.0	132.6	136.3	129.6	36.9
G_R(GPa)	77.5[a]	65.4	125.0	140.9	139.6	166.5	121.7	122.5	121.2	26.2
G_H(GPa)	79.6[a]	84.0	132.2	148.7	148.0	176.8	127.0	129.4	125.4	31.5
E_H(GPa)	209.1[a]	231.5	346.4	368.5	371.0	439.3	298.2	303.1	293.2	70.0
B_H/G_H	2.34[a]	3.76	2.30	1.58	1.69	1.61	1.20	1.19	1.18	0.95
			2.18[b]							
σ	0.31[a]	0.38	0.31	0.24	0.25	0.24	0.17	0.17	0.17	0.11
	0.29[c]		0.30[b]							
H_V(GPa)	35.82			33.39	33.39					19.23

a Cal. in Ref. [7]

b Cal. in .Ref. [4]

c Cal. in .Ref. [27]

Table 4 Anisotropic factors of Fe-P binary compounds.

E	A_1	A_2	A_3	A_B(%)	A_G(%)	A^U
Fe	2.71	2.71	2.71	0	11.45	1.29
Fe_3P	0.83	0.83	3.91	0.03	22.43	2.89
Fe_2P	1.35	1.35	1.00	0.21	5.48	0.58
o-FeP_1	1.44	1.83	0.94	3.16	5.28	0.62
o-FeP_2	0.97	1.74	1.44	4.80	5.68	0.70
FeP_2	0.72	1.05	1.17	4.42	5.80	0.71
m-FeP_4_1	0.61	0.75	1.63	0.13	4.29	0.45
o-FeP_4	0.47	1.18	1.61	0.56	5.33	0.58
m-FeP_4_2	1.41	1.30	1.66	0.03	3.35	0.35
P	0.51	2.85	0.55	27.79	16.96	2.81

Table 5 The theoretical density (ρ, g/cm^3), longitudinal sound velocity (v_l, m/s), transverse sound velocity (v_s, m/s), average sound velocity (v_m, m/s) and Debye temperature (Θ_D, K).

species	ρ	v_l	v_s	v_m	Θ_D
Fe_3P	8.343	7160.8	3173.1	3581.1	497.1
Fe_2P	5.665	9208.4	4830.8	5402.9	668.6
o-FeP_1	6.853	7955.9	4658.2	5165.0	702.1
o-FeP_2	6.853	8085.6	4647.2	5161.3	701.6
FeP_2	5.467	9752.1	5686.8	6307.8	822.4
m-FeP_4_1	4.282	8669.5	5446.0	5996.0	742.2
o-FeP_4	4.430	8580.2	5404.6	5948.6	744.7
m-FeP_4_2	4.327	8530.9	5383.4	5924.1	735.9